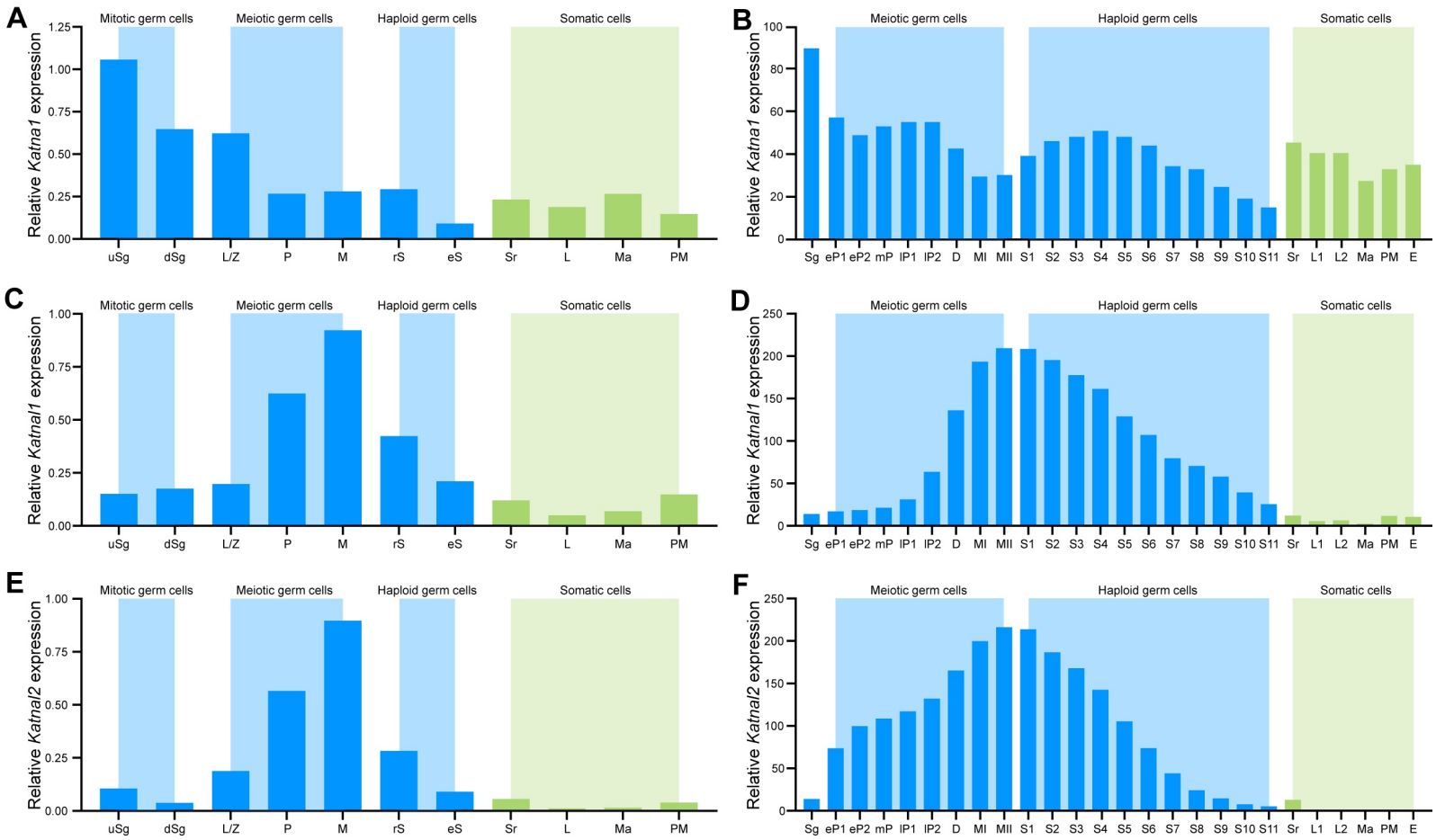

Fig. S1. Katanin A-subunit expression in the adult mouse testis.

Katna1 (**A**, **B**), *Katnal1* (**C**, **D**) and *Katnal2* (**E**, **F**) expression across major cell types in the adult mouse testis as determined by two different single-cell RNA-sequencing studies. **A**,**C**,**E** were extracted from data generated by (Jung et al., 2019) and **B**, **D**, **F** were extracted from data generated by (Ernst et al., 2019). In **A**, **C**, **E**, X-axis left to right: uSg = undifferentiated spermatogonia, dSg = differentiating spermatogonia, L/Z= leptotene/zygotene spermatocytes, P = pachytene spermatocytes, M = meiosis, rS = round spermatids, eS = elongating spermatids, Sr = Sertoli cells, L = Leydig cells, Ma = macrophages, PM = peritubular myoid cells. In **B**, **D**, **F**, X-axis left to right: Sg = spermatogonia, eP1-eP2 = early pachytene 1-2 spermatocytes, D = diplotene spermatocytes, MI = meiosis I, MII = meiosis II, S1-S11 = step 1-11 spermatids, Sr = Sertoli cell, L1-2 = Leydig cells 1-2, Ma = macrophages, PM = peritubular myoid cells, E = endothelial cells.

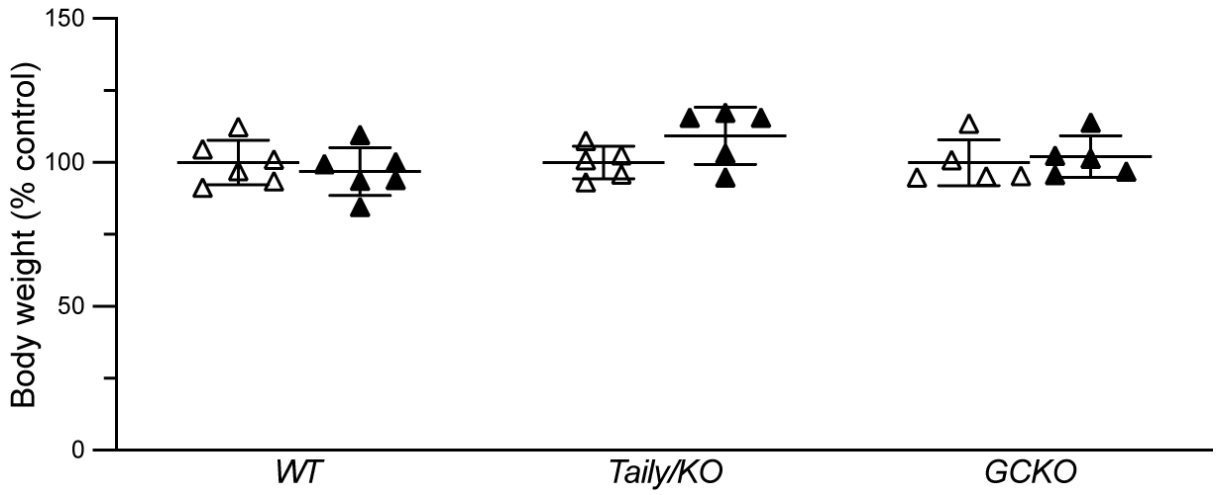

Fig. S2. Body weight of KATNB1 LOF mice.

No difference in overall body weight was observed between strain specific control male mice (white triangles) and either *Katnb1*$^{Taily/Taily}$, *Katnb1*$^{Taily/KO}$ and *Katnb1*$^{GCKO/GCKO}$ (black triangles) male mice. Lines represent mean±s.d., n=4-6 per genotype.

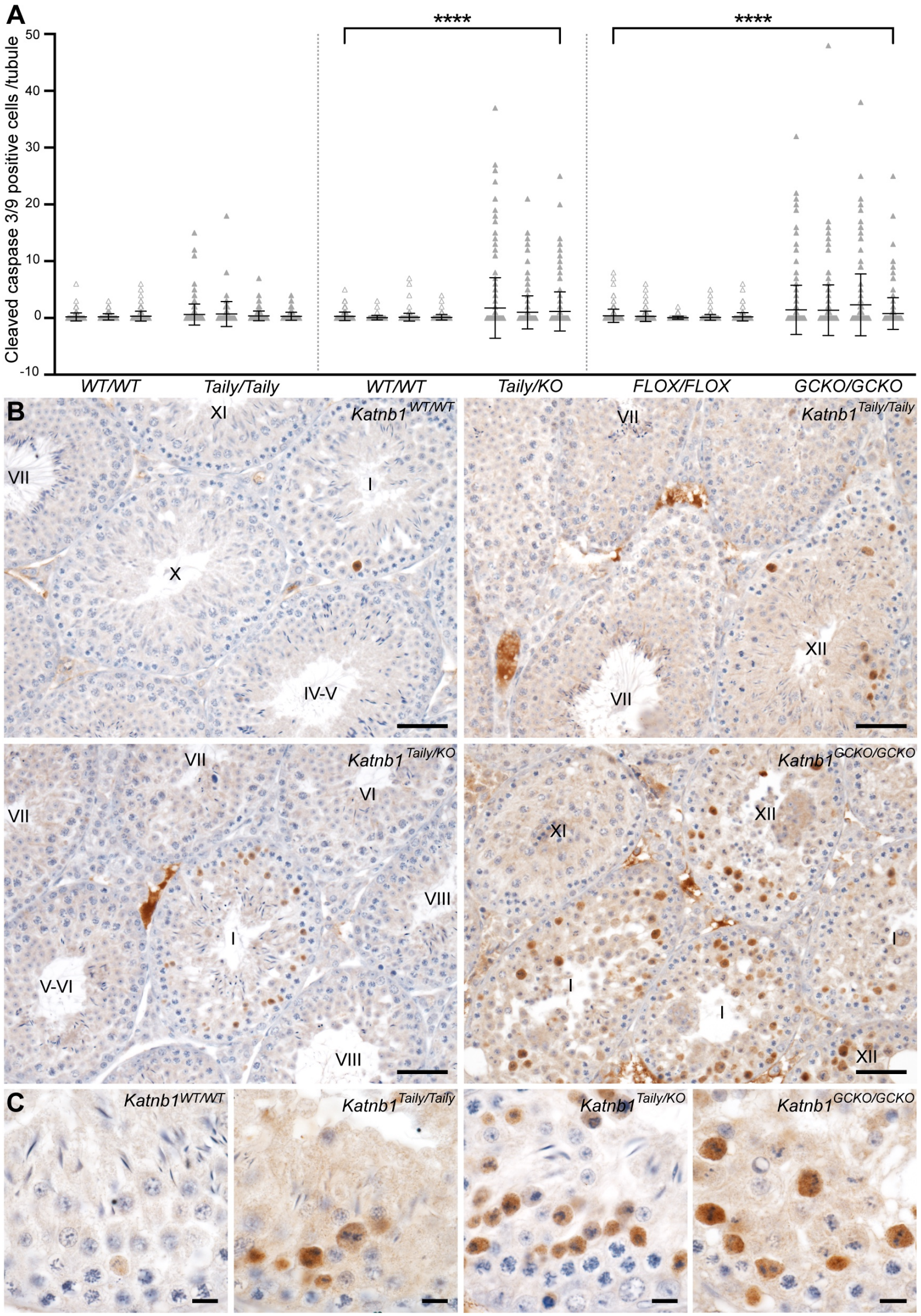

Fig. S3. Loss of KATNB1 results in increased germ cell apoptosis.

Germ cell apoptosis in KATNB1 LOF mice as assessed by immunolabelling of seminiferous tubules for cleaved-caspase 3 and 9. The average number of cleaved-caspase 3 and/or 9 positive germ cells per seminiferous tubule is graphed in (**A**) and representative images of testis immunolabelling of cleaved-caspase 3 and 9 are shown in (**B**-**C**). In (**A**) *Katnb1*$^{Taily/Taily}$, *Katnb1*$^{Taily/KO}$, *Katnb1*$^{GCKO/GCKO}$ mice (white triangles) are graphed compared to their strain specific controls (grey triangles). Sub-columns within each genotype represent individual mice, and lines represent mean±s.d. for each. A minimum of 90 randomly selected seminiferous tubules per mouse were counted (n≥3 mice /genotype). Statistically significant increases in germ cell apoptosis were observed in both *Katnb1*$^{Taily/KO}$ and *Katnb1*$^{GCKO/GCKO}$ compared to their respective controls, **** P<0.0001. Cleaved-caspase 3/9 positive cells were frequently observed in stage XII and I tubules of all KATNB1 LOF genotypes, but rarely seen in other seminiferous tubule stages or in controls (**B**). Higher magnification revealed cleaved-caspase 3/9 positive cells in *Katnb1*$^{Taily/Taily}$, *Katnb1*$^{Taily/KO}$, *Katnb1*$^{GCKO/GCKO}$ stage XII and I tubules were spermatocytes undergoing meiosis (**C**). Scale bars in **B** = 50 μm and in **A** = 10 μm. Roman numerals indicate seminiferous tubule stages in **B.**

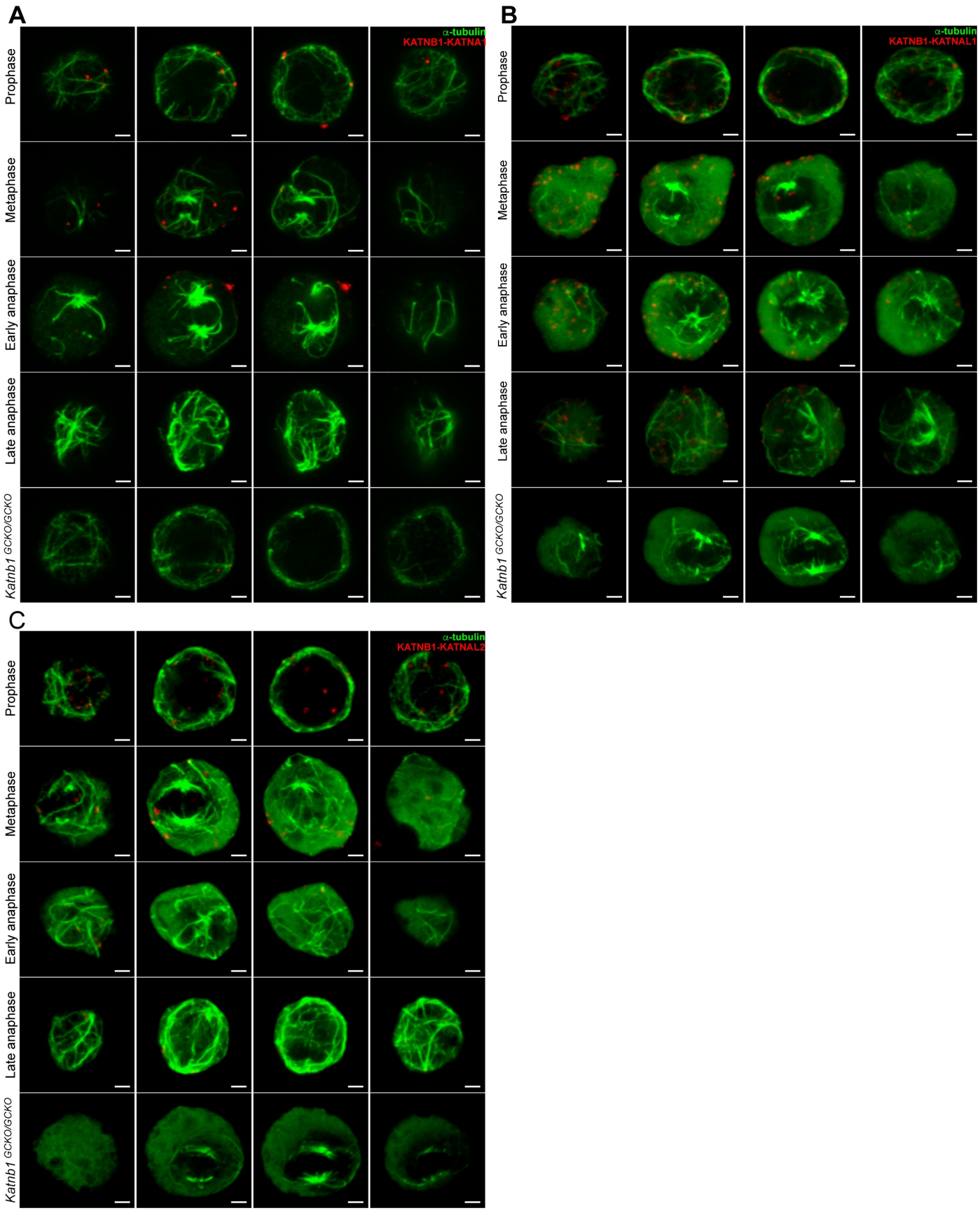

Fig. S4. Precise localisation of KATNB1-based MT severing complexes during mouse male meiosis.

Subgroups of images taken from each Z-stack presented in Fig. 4A-C to allow a more precise localisation of KATNA1-KATNB1 (**A**), KATNAL1-KATNB1 (**B**) and KATNAL2-KATNB1 (**C**) complexes during meiosis. Images represent *in situ* proximity ligation assays using antibodies directed against (**A**) KATNA1 and KATNB1, (**B**) KATNAL1 and KATNB1, and (**C**) KATNAL2 and KATNB1 in isolated *Katnb1*$^{Flox/Flox}$ spermatocytes. Assay specificity was shown by the parallel staining of *Katnb1*$^{GCKO/GCKO}$ spermatocytes. For each assay, spermatocytes from n=3 *Katnb1*$^{Flox/Flox}$ mice and from n=1 *Katnb1*$^{GCKO/GCKO}$ mouse were assessed. Red represents KATNB1-based complexes and green represents MTs as marked by α-tubulin. For each meiotic stage presented, the four images represent different depths within the same cell. Each individual image represents Z-stacks spanning 2.7 μm in the Z-plane presented as 2D maximum intensity projections. Scale bars = 2 μm.

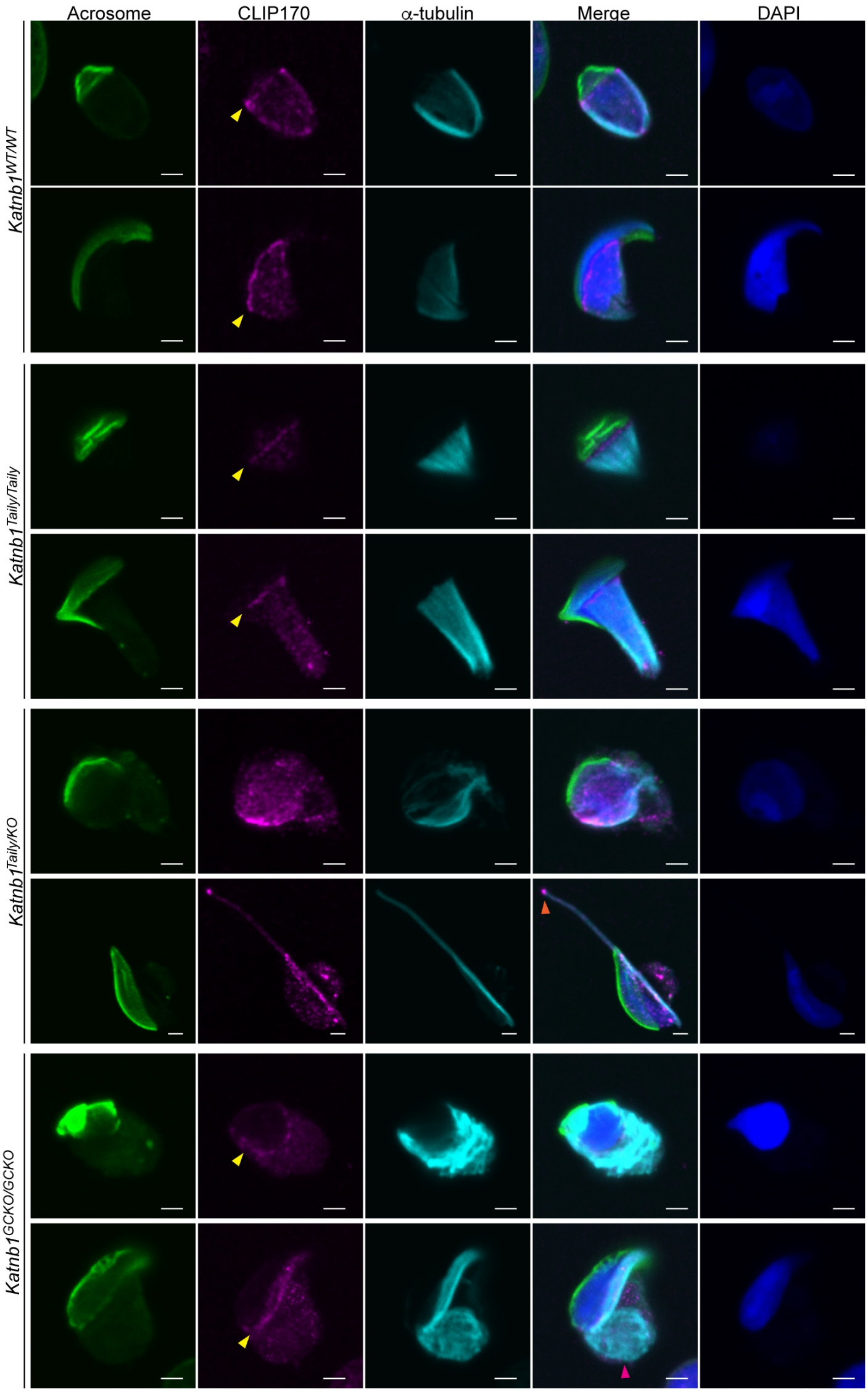
Acrosome
CLIP170
α-tubulin
Merge
DAPI
Katnb1WT/WT
Katnb1Taily/Taily
Katnb1Taily/KO
Katnb1GCKO/GCKO

Fig. S5 Perinuclear ring formation in KATNB1 LOF mice.

CLIP170 (magenta) and α-tubulin (cyan) immunolabelling as a marker of the manchette perinuclear ring/MT plus ends and of the manchette MTs respectively, in *Katnb1*$^{WT/WT}$, *Katnb1*$^{Taily/Taily}$, *Katnb1*$^{Taily/KO}$ and *Katnb1*$^{GCKO/GCKO}$ isolated spermatids. Cells were stained with PNA (green) as a marker of the acrosome and DAPI (blue) to visualise DNA. Yellow arrowheads mark the manchette perinuclear rings which formed in *Katnb1*$^{WT/WT}$, *Katnb1*$^{Taily/Taily}$ and *Katnb1*$^{GCKO/GCKO}$ spermatids. In *Katnb1*$^{Taily/KO}$ MT plus ends were not arranged into a discernible perinuclear ring structure and were instead ectopically oriented and/or located, and were arranged in small clusters (orange arrowhead). Scale bars = 2 μm.

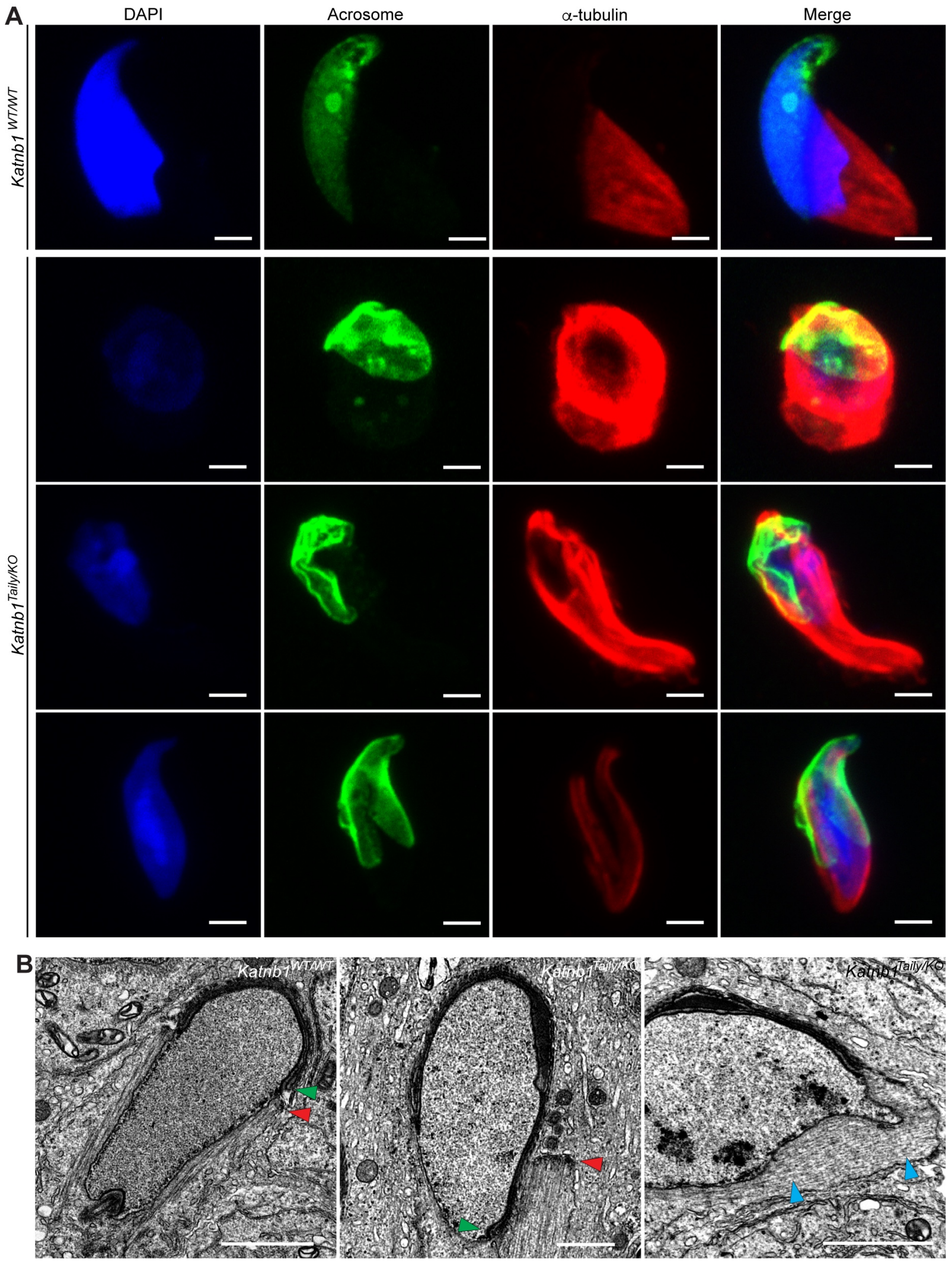

Fig. S6. *Katnb1*$^{Taily/KO}$ spermatids exhibit ectopic manchette-like MTs.

(**A**) α-tubulin immunolabelling (red) as a marker of manchette MTs, in *Katnb1*$^{WT/WT}$ and *Katnb1*$^{Taily/KO}$ isolated spermatids. Cells were counterstained with FITC-PNA (green) as a marker of acrosomes and DAPI (blue) to visualise DNA. Scale bars = 2 μm. (**B**) TEM of *Katnb1*$^{WT/WT}$ and *Katnb1*$^{Taily/KO}$ step 10 spermatids. In *Katnb1*$^{WT/WT}$ mice during sperm head shaping the manchette perinuclear ring (red arrowhead) was always located immediately distal to the leading edge of the acrosome (green arrowhead) and manchette MTs were always oriented in parallel to the long axis of the cell. In *Katnb1*$^{Taily/KO}$ spermatids the perinuclear ring was frequently not observed or ectopic fragments of perinuclear and manchette MTs (red arrowheads) were observed, which were neither situated distal to the acrosome leading edge (green arrowhead) nor associated with the nucleus. In *Katnb1*$^{Taily/KO}$ spermatids manchette-like MTs (blue arrowheads) incorrectly oriented along the long axis of the cell were also frequently observed. Scale bars = 2 μm.

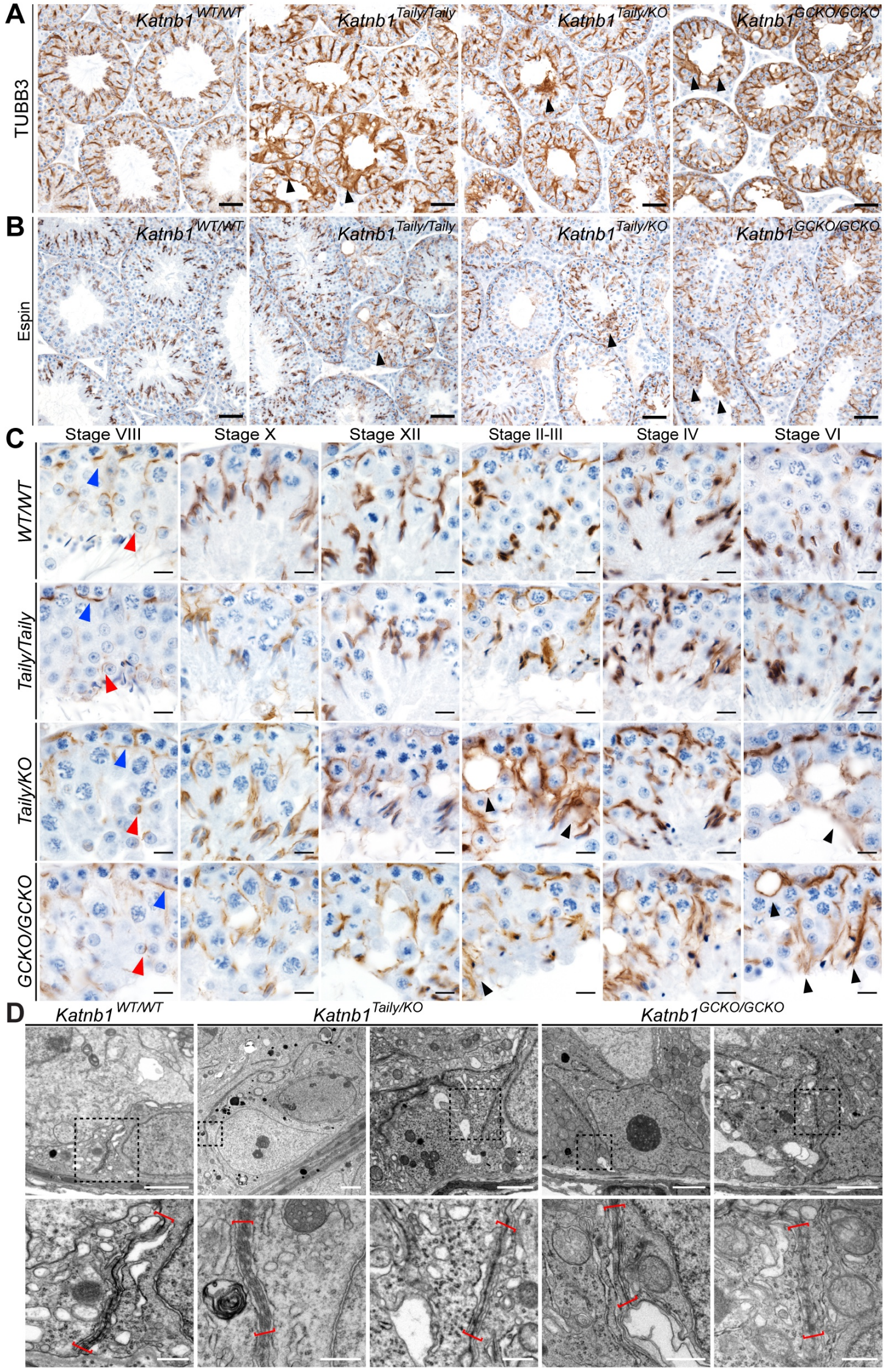

Fig. S7. The Sertoli cell cytoskeleton is disrupted in all three KATNB1 LOF models Testis sections immunolabelled with TUBB3 (**A)** as a marker of Sertoli cell specific MTs and espin (**B,C**) as a marker of ES junctions in KATNB1 LOF mice. TUBB3 immunolabelling (**A**) revealed disorganisation of the Sertoli cell cytoskeleton in *Katnb1*$^{Taily/Taily}$, *Katnb1*$^{Taily/KO}$ and *Katnb1*$^{GCKO/GCKO}$ mice compared to controls. Abnormal enrichment of Sertoli cell MTs (black arrowheads) was observed in areas of *Katnb1*$^{Taily/Taily}$, *Katnb1*$^{Taily/KO}$ and *Katnb1*$^{GCKO/GCKO}$ seminiferous epithelium devoid of germ cells and around pyknotic germ cells. Espin immunolabelling (**B,C)** revealed basal ES junctions (blue arrowheads) were overtly normal in KATNB1 LOF mice compared to controls. Apical ESs formed normally in KATNB1 LOF mice at stage VIII between step 8 spermatids and Sertoli cells (**C**, red arrowheads), however as spermiogenesis progressed ectopic tracts of ES accumulated in disorganised areas of seminiferous epithelium and at sites of germ cell loss (**B,C**, black arrowheads). Scale bars **A**,**B** = 50 μm, **C** = 10 μm. TEM of the basal ES of the blood-testis-barrier in *Katnb1*$^{WT/WT}$, *Katnb1*$^{Taily/KO}$ and *Katnb1*$^{GCKO/GCKO}$ mice (**D**). Lower panels (scalebars = 0.5 μm) correspond to higher magnification images of upper panels (scalebars = 2 μm). Red brackets indicate the basal ES.

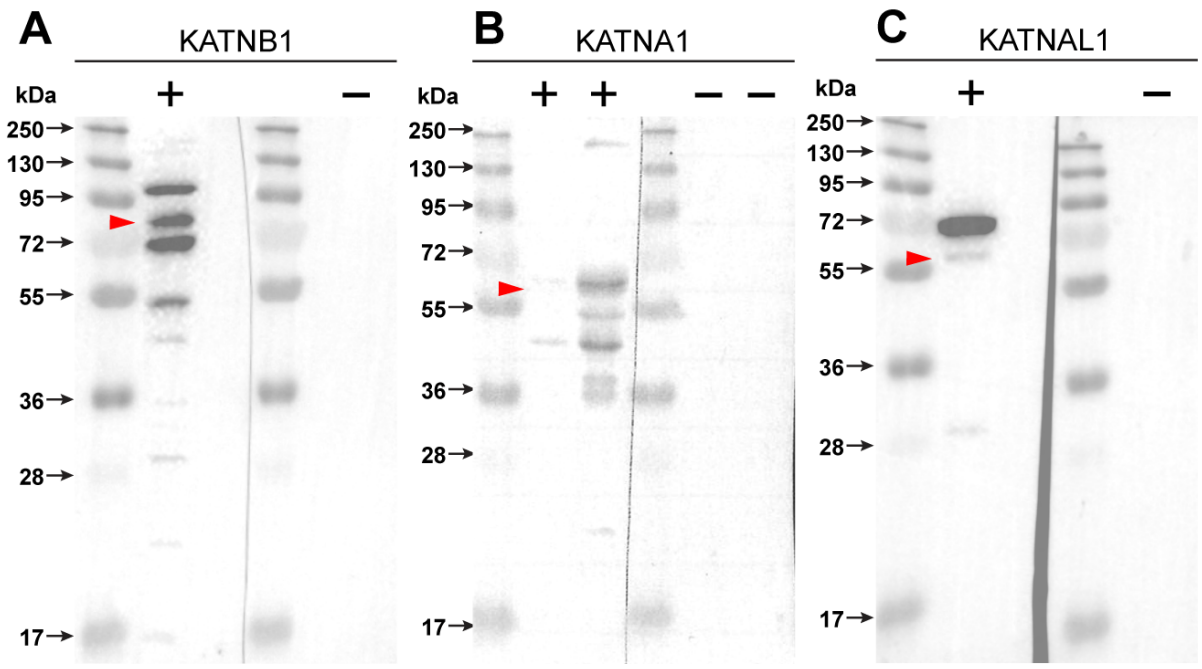

Fig. S8. Validation of the KATNB1, KATNA1 and KATNAL1 antibodies.

Specificity of the KATNB1 (**A**), KATNA1 (**B**) and KATNAL1 (**C**) antibodies was determined by pre-absorption of each with a molar excess of the corresponding immunising peptide prior to immuno-detection on whole adult mouse testes homogenates. Positive control immunoblots for each antibody (+) were conducted in parallel and compared to the pre-absorption controls (-). Red arrowheads indicate the predicted size of the canonical isoform of each protein.